

Interactive 3D Medical Image Segmentation with SAM 2

Chuyun Shen^{*†}

*School of Computer Science and Technology
East China Normal University
Shanghai 200062, China*

CYSHEN@STU.ECNU.EDU.CN

Yifei Huang[†]

*School of Software Engineering
East China Normal University
Shanghai 200062, China*

HYIFEI_YOF@163.COM

Wenhao Li

*School of Software Engineering
Shanghai Research Institute for Intelligent Autonomous Systems
Tongji University
Shanghai 200092, China*

WHLI@TONGJI.EDU.CN

Yuhang Shi

*Shanghai United Imaging Healthcare Advanced Technology
Research Institute Co., Ltd.
Shanghai 201807, China*

YUHANG.SHI@CRI-UNITED-IMAGING.COM

Xiangfeng Wang

*School of Computer Science and Technology
East China Normal University
Shanghai 200062, China*

XFWANG@CS.ECNU.EDU.CN

Abstract

Interactive medical image segmentation (IMIS) has shown significant potential in enhancing segmentation accuracy by integrating iterative feedback from medical professionals. However, the limited availability of enough 3D medical data restricts the generalization and robustness of most IMIS methods. The Segment Anything Model (SAM), though effective for 2D images, requires expensive semi-auto slice-by-slice annotations for 3D medical images. In this paper, we explore the zero-shot capabilities of SAM 2, the next-generation Meta SAM model trained on videos, for 3D medical image segmentation. By treating sequential 2D slices of 3D images as video frames, SAM 2 can fully automatically propagate annotations from a single frame to the entire 3D volume. We propose a practical pipeline for using SAM 2 in 3D medical image segmentation and present key findings highlighting its efficiency and potential for further optimization. Concretely, numerical experiments on the BraTS2020 and the medical segmentation decathlon datasets demonstrate that SAM 2 still has a gap with supervised methods but can narrow the gap in specific settings and organ types, significantly reducing the annotation burden on medical professionals. Our code will be open-sourced and available at https://github.com/Chuyun-Shen/SAM_2_Medical_3D.

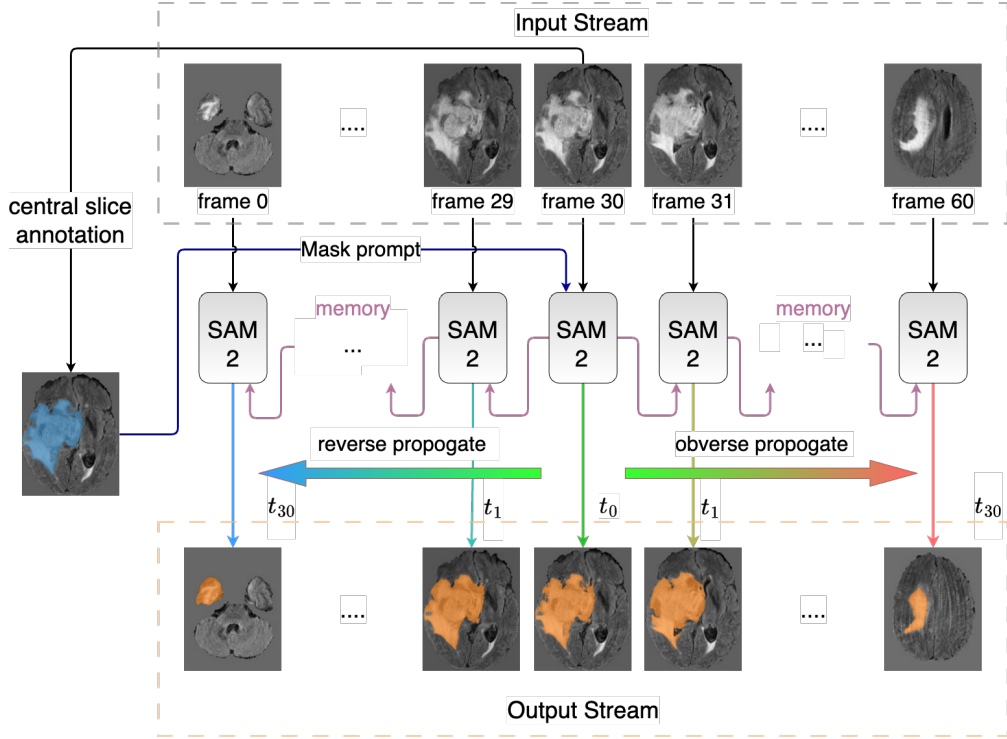


Figure 1: Pipeline Diagram: Utilizing Sam 2 for Propagating Slice Annotations for 3D Interactive Medical Image Segmentation. The central slice first needs to be segmented by a 2D segmentation algorithm or annotated by a human expert either through manual labeling or using an interactive semi-automatic algorithm. SAM 2 inputs the mask prompt and then predicts all other slices sequentially in both directions, ultimately obtaining annotations for all slices.

1. Introduction

Medical image segmentation (MIS) (Ronneberger et al., 2015; Isensee et al., 2021; Zhou et al., 2021; Cao et al., 2023) poses distinct challenges compared to natural images due to the diverse modalities, intricate anatomical structures, unclear and complex object boundaries, and varying object scales involved (Sharma and Aggarwal, 2010; Hesamian et al., 2019; Huang et al., 2023). Thus, the interactive medical image segmentation (IMIS) paradigm has garnered significant attention for substantially improving performance over conventional methods (Xu et al., 2016; Rajchl et al., 2016; Lin et al., 2016; Castrejon et al., 2017; Wang et al., 2018; Song et al., 2018; Liao et al., 2020a; Ma et al., 2021; Li et al., 2021).

IMIS reimagines MIS as a multi-stage, human-in-the-loop process, where medical professionals provide iterative feedback—such as marking critical points, delineating boundaries, or defining bounding boxes—to refine model outputs. This iterative feedback loop allows the model to integrate expert knowledge and progressively enhance segmentation accuracy.

*. This work was finished during an internship at Shanghai United Imaging Healthcare Advanced Technology.

†. These authors contributed equally to this work.

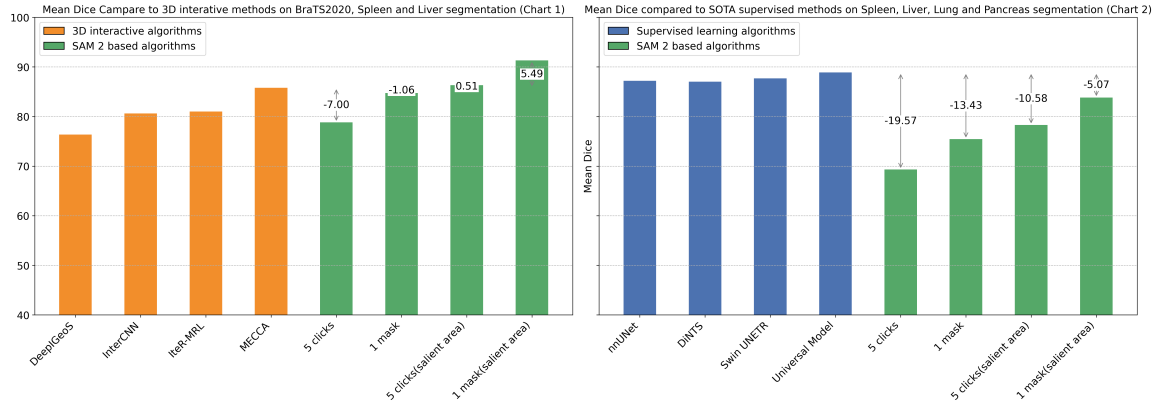


Figure 2: Comparison with 3D interactive methods and supervised methods. The orange bars represent 3D interactive algorithms, which typically handle 3D images by resizing. The blue bars denote supervised learning algorithms, which usually process 3D images using patches. The green bars signify algorithms based on SAM 2 segmentation. In this context, "5 clicks" refers to interactively clicking on five points on the central 2D image using SAM, one point per round, to generate 2D slice annotations, which are then propagated to the 3D image. "1 mask" indicates providing SAM 2 with the ground truth mask of the central 2D image, which is then propagated to the 3D image. "Salient area" refers to results tested only on slices with more than 256 foreground points. The bidirectional arrows indicate the difference in dice score between SAM 2-based algorithms and the optimal algorithms. Chart 1 compares the dice scores of 3D interactive algorithms and SAM 2 on the BraTS2020, Spleen, and Liver datasets, while Chart 2 compares the dice scores of supervised algorithms and SAM 2 on the Spleen, Liver, Lung, and Pancreas datasets.

However, the limited availability of medical data restricts most IMIS methods to a few datasets and segmentation tasks, resulting in poor generalization and robustness.

The *Segment Anything Model* (SAM) (Kirillov et al., 2023) has shown exceptional effectiveness in interactive segmentation for natural images and, more recently, medical images, thanks to its prompt-based, zero-shot generalization capabilities (Ji et al., 2023a,b; Mohapatra et al., 2023; Deng et al., 2023; Zhou et al., 2023; He et al., 2023a; Mazurowski et al., 2023; Ma and Wang, 2023; Cheng et al., 2023; Zhang and Jiao, 2023; Roy et al., 2023; Huang et al., 2023; Mattjie et al., 2023). Despite this, SAM’s training on 2D natural images presents a significant mismatch with the 3D nature of medical imaging modalities like CT, MRI, and PET. Current SAM-based tools require laborious slice-by-slice annotations, even for similar slices, which is impractical in clinical settings.

Fortunately, SAM 2 (Ravi et al., 2024), the next generation of Meta SAM trained on videos, offers a promising solution. SAM 2 can segment entire videos based on annotations from a *single* frame, utilizing interactions (clicks, boxes, or masks) on any frame to predict spatiotemporal masks, or ‘masklets.’ Different slices of 3D medical images are sequentially scanned and stacked over time, allowing 3D medical images to be naturally regarded as videos. This naturally raises the following question:

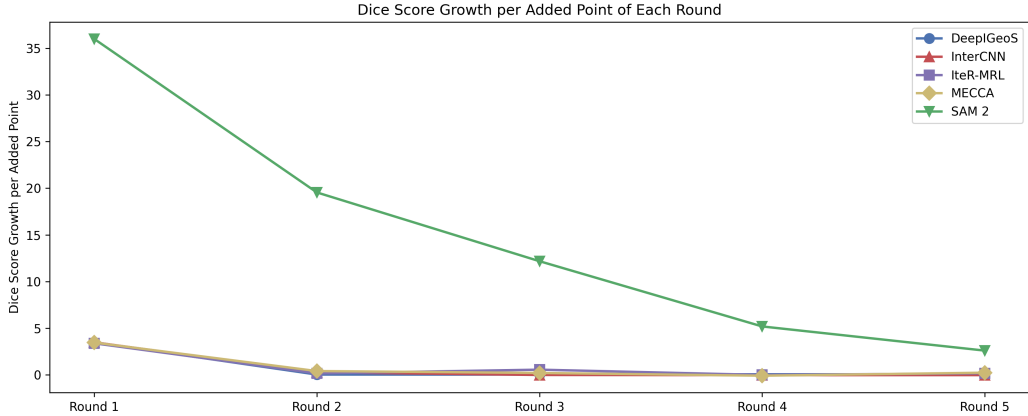


Figure 3: Dice Score Growth per Added Point of Each Round: On the BraTS2020 benchmark, we evaluated how much the average dice score improves per additional point in each round for different interactive algorithms. The interactive methods used by the four algorithms—DeepIGeoS, InterCNN, IteR-MRL, and MECCA—select 25 points in the first round on the 3D medical image, followed by 5 additional points per round. In contrast, our pipeline with SAM 2 adds one point per round.

Can SAM 2 segments 3D medical image based solely on 2D interactive feedbacks in a zero-shot manner?

If we can get an affirmative answer, this paradigm shift could enable researchers to focus on automatic segmentation for single 2D images, thus significantly reducing the amount of expert annotation required for 3D interactive segmentation. This paper attempts to preliminarily answer this question from an experimental perspective and has obtained some dialectical observations. Concretely, we propose a simple and practical pipeline (Shown in Fig.1) to enable the use of SAM 2 for 3D medical images, evaluate SAM 2’s zero-shot performance on the Brats and some MSD datasets, and get the following key observations: (1) The experimental results suggest that SAM 2, in a zero-shot manner, still has a gap with supervised methods but can narrow the gap in specific settings and organ types (shown in Fig.2). Further optimization and refinement of the medical 3D images is necessary. (2) SAM 2’s efficiency in utilizing interactive feedback significantly surpasses that of other 3D interactive medical image segmentation algorithms. (shown in Fig.3)

Remark. Since the release of SAM 2, two works have explored its application in medical image segmentation. Dong et al. (2024) introduce SAM 2 for 3D Medical Imaging by treating each slice as a frame and leveraging a memory bank for prediction propagation. They conduct an extensive evaluation of SAM 2 using 18 diverse medical imaging datasets, demonstrating its performance in both single-frame 2D segmentation and multi-frame 3D segmentation. They also identify key strategies for enhancing SAM 2’s segmentation accuracy, including selecting the center slice of the object of interest, utilizing bidirectional propagation, and preferring the first predicted mask over the most confident one. Another notable work, the MedSAM-2 Framework (Zhu et al., 2024), represents the first SAM-2-based model for medical image segmentation, addressing both 2D and 3D tasks. MedSAM-2 incorporates the Confidence Memory Bank and Weighted Pick-up strategy, surpassing state-of-the-art

models across 15 benchmarks and 26 tasks, thereby demonstrating superior generalization and performance. In contrast to these studies, our work does not explore different modes; rather, it adopts settings specifically tailored for medical imaging, akin to the optimal strategy mentioned in Dong et al. (2024). We also discussed and investigated the feasibility of interactive annotation based on SAM 2 on 2D slices, subsequently propagating these annotations to 3D images. Additionally, we compared the accuracy of this method with traditional 3D interactive medical image segmentation algorithms and supervised learning algorithms, highlighting the gap in performance with them.

2. Related Work and Preliminaries

2.1 3D Interactive Medical Image Segmentation

In recent years, deep learning-based interactive medical image segmentation (IMIS) methods have garnered significant interest. Xu et al. (2016) proposed using convolutional neural networks (CNNs) for interactive image segmentation. Techniques like DeepCut (Rajchl et al., 2016) and ScribbleSup (Lin et al., 2016) leverage weak supervision to develop interactive segmentation approaches. Additionally, DeepIGeoS (Wang et al., 2018) incorporates a geodesic distance metric to create a hint map for improved segmentation accuracy.

The sequential nature of the interactive segmentation process makes it well-suited for reinforcement learning (RL). Polygon-RNN (Castrejon et al., 2017) addresses this by treating segmentation targets as polygons and iteratively selecting polygon vertices via a recurrent neural network (RNN). Similarly, Polygon-RNN+ (Acuna et al., 2018) employs RL to enhance vertex selection further. SeedNet (Song et al., 2018) takes a distinct approach by developing an RL model for expert interaction generation, enabling the acquisition of simulated interaction data at each stage of the segmentation process. IteR-MRL (Liao et al., 2020a) and BS-IRIS (Ma et al., 2021) frame the dynamic interaction process as a Markov Decision Process (MDP), utilizing multi-agent RL models for image segmentation. Building on IteR-MRL, MECCA (Li et al., 2021) introduces a confidence network to address the common issue of "interactive misunderstanding" in RL-based IMIS techniques and to enhance the utilization of human feedback. Additionally, Marinov et al. (2023) provides a thorough review of the IMIS domain. These advancements underscore the potential of deep learning and reinforcement learning in revolutionizing interactive medical image segmentation, leading to more accurate and efficient segmentation techniques.

2.2 Segment Anything Model and Segment Anything Model 2

The *Segment Anything Model* (SAM) (Kirillov et al., 2023) and its successor, the *Segment Anything Model 2* (SAM 2) (Ravi et al., 2024), introduced by Meta, are significant advancements in image and video segmentation. These models aim to provide a unified framework for segmentation tasks, drawing inspiration from foundational models in NLP and CV. SAM focuses on image segmentation using promptable tasks to generate valid masks based on user-defined prompts. SAM 2 extends these capabilities to video segmentation, addressing challenges such as object motion and deformation.

Model. SAM's architecture includes an image encoder for embeddings, a prompt encoder, and a mask decoder to integrate inputs and predict masks. SAM 2 enhances SAM's architecture

with video processing capabilities. It introduces a temporal component for handling video frames, generating spatio-temporal masks (masklets) to track objects across frames.

Data. SAM is trained on the SA-1B dataset, containing over 1 billion masks from 11 million images, ensuring robust generalization. SAM 2 extends the dataset to include annotated video sequences, allowing it to learn from dynamic scenes and temporal changes.

Task. SAM’s promptable segmentation task generates masks based on prompts that define target objects within an image, producing plausible masks even for ambiguous prompts. SAM 2 expands this task to video data, generating masklets that track objects across frames, maintaining accuracy despite object motion and varying conditions.

In summary, SAM addresses image segmentation, while SAM 2 extends capabilities to video segmentation. For comprehensive details, refer to the primary publications (Kirillov et al., 2023; Ravi et al., 2024) and relevant surveys (Zhang et al., 2023).

2.3 Segment Anything in Medical Images

Leveraging the foundational pre-trained models of SAM, various studies have investigated its effectiveness in diverse zero-shot medical imaging segmentation (MIS) scenarios. For instance, Ji et al. (2023a) performed an extensive evaluation of SAM in the *everything* mode for segmenting lesion regions in different anatomical structures (e.g., brain, lung, and liver) and imaging modalities (CT and MRI).

Further, Ji et al. (2023b) analyzed SAM’s performance in specific medical fields, such as optical disc and cup, polyp, and skin lesion segmentation. They used both the automatic *everything* mode and the manual *prompt* mode, employing points and bounding boxes as prompts.

In the context of MRI brain extraction, Mohapatra et al. (2023) compared SAM’s performance to the well-known *Brain Extraction Tool* (BET) from the *FMRIB Software Library*. Additionally, Deng et al. (2023) evaluated SAM’s capabilities in digital pathology segmentation tasks, including the segmentation of tumor, non-tumor tissue, and cell nuclei in high-resolution whole-slide images. Zhou et al. (2023) applied SAM to polyp segmentation tasks using five benchmark datasets under the *everything* setting.

Recently, multiple studies have rigorously assessed SAM on over ten publicly available MIS datasets or tasks (He et al., 2023a; Mazurowski et al., 2023; Ma and Wang, 2023; Wu et al., 2023; Huang et al., 2023; Zhang and Liu, 2023). Moreover, Liu et al. (2023) integrated SAM with the *3D Slicer* software to facilitate the design, evaluation, and application of SAM in medical imaging segmentation.

Quantitative experimental results from these studies suggest that SAM’s zero-shot performance is generally moderate and varies across different datasets and tasks. Specifically: 1. Using the *prompt* mode instead of the *everything* mode, SAM can exceed state-of-the-art (SOTA) performance in tasks involving large objects, smaller quantities, and well-defined boundaries, especially with dense human feedback. 2. However, a significant performance gap exists between SAM and SOTA methods in tasks involving dense and amorphous object segmentation. 3. It is also important to note that most deep learning-based MIS methods require retraining from scratch for specific subtasks, and SAM-based methods are primarily limited to 2D images.

3. Experiments and Results

In this study, we primarily aim to explore whether annotations made on 2D medical slices using SAM 2 can be extended to entire 3D slices. If feasible, this could significantly reduce the annotation cost for physicians. To ensure the generalizability of our experimental results, we have selected two datasets: Brats2020 (Menze et al., 2014) and the medical segmentation decathlon (MSD) (Antonelli et al., 2022). These datasets include MRI and CT images and encompass various commonly used medical organs and lesions.

3.1 Datasets

In this work, we primarily experiment with SAM 2 on two datasets: BraTS2020 and MSD.

The BraTS2020 dataset is part of the Brain Tumor Segmentation Challenge, focusing on the segmentation of gliomas in pre-operative MRI scans. It includes multimodal scans available as NIfTI files, covering native (T1), post-contrast T1-weighted (T1Gd), T2-weighted (T2), and T2 Fluid Attenuated Inversion Recovery (T2-FLAIR) volumes. We chose T2-FLAIR as our input 3D image modality because it is particularly effective in highlighting differences between normal and abnormal brain tissue, making it ideal for identifying and segmenting brain tumors. Our target is to segment the entire tumor area, including the enhancing tumor, the peritumoral edema, and the necrotic core.

The Medical Segmentation Decathlon (MSD) dataset is another significant resource designed to evaluate generalizable algorithms across various medical image segmentation tasks. It includes diverse imaging modalities and anatomical structures, such as MRI and CT scans of different organs. We utilized several tasks from MSD to segment specific organs: Task03_Liver: Focuses on segmenting liver structures in CT images, identifying the liver. Task06_Lung: Aims to segment lung regions in CT scans. Task07_Pancreas: Involves segmenting the pancreas in CT images. Task09_Spleen: Targets the segmentation of the spleen in CT scans.

These tasks help develop and benchmark robust segmentation algorithms across different medical imaging modalities.

3.2 Evaluation Metrics

In our experiments, we utilize the Dice coefficient and the 95% Hausdorff distance (HD) as evaluation metrics:

- **Dice Coefficient** (Dice, 1945): The Dice coefficient is a measure of similarity between two sets, often used to gauge the accuracy of segmentation. It is calculated as follows:

$$\text{Dice}(X, Y) = \frac{2 \cdot \|X \cap Y\|_1}{\|X\|_1 + \|Y\|_1}. \quad (1)$$

A higher Dice coefficient indicates a greater overlap between the predicted segmentation and the ground truth, reflecting a more accurate segmentation result.

- **Normalized Surface Dice (NSD)** (DeepMind, 2018): The Normalized Surface Dice (NSD) is a metric that quantifies the similarity between two sets of points, typically surfaces in a three-dimensional space. The NSD is defined as:

$$\text{NSD}(X, Y) = \frac{|\{x \in X \mid d(x, Y) \leq \delta\} \cap \{y \in Y \mid d(y, X) \leq \delta\}|}{|X| + |Y|}, \quad (2)$$

where $d(a, B)$ represents the minimum Euclidean distance from point a to set B , and δ is a predefined distance threshold. This metric effectively measures the proportion of surface points from one set within a specified distance δ of the other set's surface points, normalized by the total number of surface points in both sets. The NSD score ranges from 0 to 1, where a score closer to 1 indicates higher similarity between the two surfaces.

3.3 Main Results

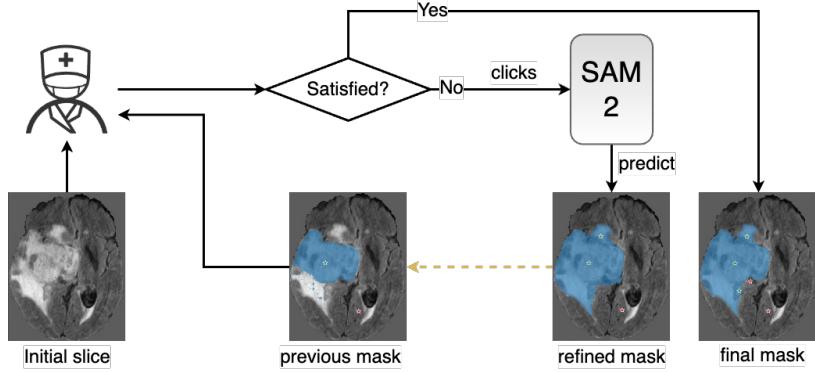


Figure 4: Interactive segmentation on a slice with SAM 2.

In this section, we present the performance of SAM 2 under different datasets and different settings. Our experiment loads the ‘sam2_hiera_large’ checkpoint and mainly focuses on two settings. The first involves multiple rounds of interaction on a single slice before propagating to the entire 3D image (shown in Fig.4). The second setting involves annotating a single slice and then propagating it to the entire 3D image.

3.3.1 COMPARED WITH STATE-OF-THE-ART METHODS

We compare the performance of SAM 2 with several state-of-the-art 3D interactive segmentation methods, including DeepIGeoS, InterCNN, IteR-MRL, and MECCA, on the BraTS2020, Spleen, and Liver datasets. As shown in Table 1 and 2, SAM 2 was tested under different configurations: with five interactive clicks (5 clicks) and a single ground truth mask (1 mask), both with and without focusing on the salient area.

To be noticed, these state-of-the-art 3D interactive segmentation methods are trained in resized image schema as 3D images in their original size are always too large to be loaded for training. Also, the resized schema needs no extra process for human feedback, as the whole image can be input into the networks. The results indicate that while SAM 2 generally lags behind the best-performing methods for BraTS and Spleen, it shows a significant improvement in the Liver dataset. Notably, using the "1 mask" setting in the salient area for the Liver dataset, SAM 2 surpasses the best results by a considerable margin.

Table 1: Comparison with 3D interactive medical image segmentation methods on BraTS2020, Spleen, and Liver segmentation tasks. “SAM 2 (5 clicks)” refers to interactively clicking on five points on the central 2D image using SAM, one point per round, to generate 2D slice annotations, which are then propagated to the 3D image. “SAM 2 (1 mask)” indicates providing SAM 2 with the ground truth mask of the central 2D image, which is then propagated to the 3D image. “Salient area” refers to results tested only on slices with more than 256 foreground points. The symbols in the following table represent the same meaning. We use bold to indicate the best result.

Method	BraTS	Spleen	Liver
DeepIGeoS (Wang et al., 2018)	88.54	91.97	48.57
InterCNN (Bredell et al., 2018)	88.39	93.52	59.92
IteR-MRL (Liao et al., 2020b)	89.22	91.50	62.29
MECCA (Shen et al., 2023)	91.02	94.96	71.46
SAM 2 (5 clicks)	75.52	79.59	81.32
Compared with the best results	-17.03%	-16.19%	13.80%
SAM 2 (1 mask)	81.29	82.77	90.18
Compared with the best results	-10.69%	-12.84%	26.20%
SAM 2 (5 clicks) (salient area)	81.12	92.98	84.85
Compared with the best results	-10.88%	-2.09%	18.74%
SAM 2 (1 mask) (salient area)	87.17	94.41	92.33
Compared with the best results	-4.23%	-0.58%	29.21%

SAM 2 is also evaluated against several supervised methods, including nnUNet, DiNTS, Swin UNETR, and Universal Model, across different organ segmentation tasks: Spleen, Liver, Lung, and Pancreas, as presented in Table 2. Different from the resize schema, which is commonly used in 3D interactive medical image segmentation, these methods are trained with patches. Patch-based training can keep the origin resolution without losing any details, which ensures high segmentation accuracy.

To be noticed the results of the supervised method are obtained from the MSD public leaderboard. The zero-shot method based on SAM 2 was tested on the training set. Since it was trained on a natural image dataset, there is no risk of data leakage. We must acknowledge that there may be slight differences in the distribution of the test dataset. However, for the SAM 2-based algorithm, all datasets used are unseen, and we believe this difference is negligible.

The results demonstrate that SAM 2, in its various configurations, achieves competitive performance. we can see that there is a difference of 10.5% to 64.81% between SAM 2 (5 clicks) and SOTA. The difference for SAM 2 (1 mask) is relatively smaller, ranging from 3.29% to 57.84%. Particularly, when tested on salient areas, SAM 2 performs comparably to the best results for Spleen and Liver segmentation. However, its performance varies more significantly for Lung and Pancreas segmentation tasks.

Overall, as shown in Fig.2, we have averaged these results for a clear comparison. the experimental results suggest that SAM 2 still has a gap with supervised methods and can narrow the gap in specific settings and organ types. Further optimization and refinement of the medical 3D images is necessary.

Table 2: Comparison with supervised methods for various organs.

Method	Spleen		Liver		Lung		Pancreas	
	Dice	NSD	Dice	NSD	Dice	NSD	Dice	NSD
nnUNet (Isensee et al., 2021)	97.43	99.89	95.75	98.55	73.97	76.02	81.64	96.14
DiNTS (He et al., 2023b)	96.98	99.83	95.35	98.69	74.75	77.53	81.02	96.26
Swin UNETR (Tang et al., 2024)	96.99	99.84	95.35	98.34	76.60	77.40	81.85	96.57
Universal Model (Liu et al., 2024)	97.27	99.87	95.42	98.18	80.01	81.25	82.84	96.65
SAM 2 (5 clicks)	79.59	75.63	81.32	50.47	71.61	68.99	44.73	34.01
Compared with the best results	-18.31%	-24.29%	-15.07%	-48.86%	-10.50%	-15.09%	-46.00%	-64.81%
SAM 2 (1 mask)	82.77	79.35	90.18	61.29	77.38	74.97	51.48	40.75
Compared with the best results	-15.05%	-20.56%	-5.82%	-37.90%	-3.29%	-7.73%	-37.86%	-57.84%
SAM 2 (5 clicks)(salient area)	92.98	89.71	84.85	52.69	83.93	78.68	51.45	40.82
Compared with the best results	-4.57%	-10.19%	-11.38%	-46.61%	4.90%	-3.16%	-37.89%	-57.77%
SAM 2 (1 mask)(salient area)	94.41	92.46	92.33	63.13	87.48	82.39	61.04	50.65
Compared with the best results	-3.10%	-7.44%	-3.57%	-36.03%	9.34%	1.40%	-26.32%	-47.59%

3.3.2 STATISTICS OF IMPROVEMENT BROUGHT ABOUT BY INTERACTION

SAM 2, benefiting from the SA-V dataset, which comprises 50.9K videos and 642.6K masklets, and its carefully designed architecture, demonstrates robust zero-shot inference capabilities on natural images. We evaluated the performance of SAM 2 on the BraTS2020 benchmark and compared it with 3D interactive medical segmentation algorithms.

The algorithms DeepIGeoS, InterCNN, IteR-MRL, and MECCA adopt direct clicks on 3D medical images over five rounds, with 25 interaction points provided in the first round and 5 additional points in each subsequent round. For SAM 2, we employed a similar setup; however, interactions were conducted on 2D slices with only one point per round, which SAM 2 then propagates to the entire 3D image.

To fairly compare the algorithms’ utilization of interactive feedback, we selected the Dice Score Growth per Added Point, which is the increase in dice score during a round divided by the number of new points added. As shown in Figure 3, SAM 2’s efficiency in utilizing interactive feedback significantly surpasses that of other algorithms. This demonstrates that SAM 2 possesses strong refinement capabilities based on interactions in the medical imaging domain.

Additionally, we assessed the discrepancy between slice annotations obtained through multiple rounds of interactive clicks and the slice ground truth. As shown in Figure 5, performance gradually improves and approaches the ground truth with an increasing number of clicks. This further validates the feasibility of interactive 2D slice segmentation followed by propagation using SAM 2.

4. Conclusion

In this paper, we investigated the application of the Segment Anything Model 2 (SAM 2) for zero-shot 3D medical image segmentation. By leveraging its ability to propagate annotations from a single 2D slice to an entire 3D volume, SAM 2 addresses the limitation of traditional 2D trained models that they struggle with 3D medical images because they

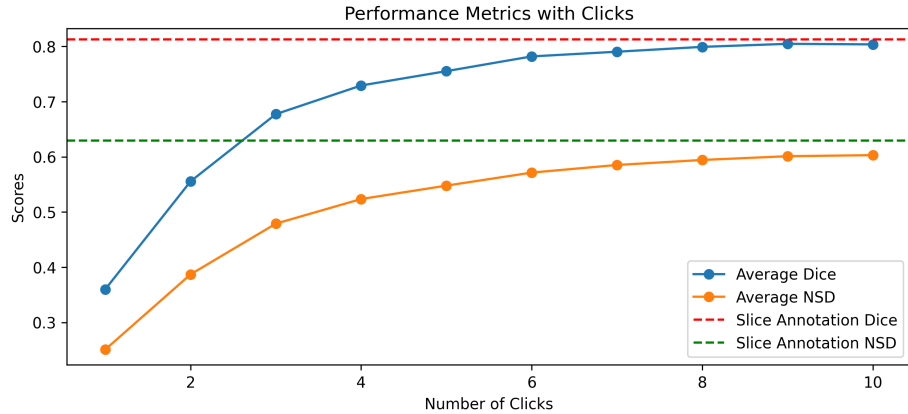


Figure 5: SAM 2 with different iterative steps on Brats2020 benchmark.

can't efficiently use the features and annotations from one slice across other slices. Our experiments on the BraTS2020 and MSD datasets reveal that SAM 2, while not yet matching the performance of specialized supervised methods, shows promising results in specific settings and organ types. The efficiency of SAM 2 in utilizing interactive feedback surpasses that of other 3D interactive segmentation algorithms, demonstrating its potential to significantly reduce the annotation workload for medical professionals. However, further optimization and refinement are necessary to enhance its performance and generalizability. This empirical study lays the groundwork for future research into leveraging advanced models like SAM 2 to revolutionize 3D medical image segmentation, ultimately improving clinical workflows and patient outcomes.

References

- David Acuna, Huan Ling, Amlan Kar, and Sanja Fidler. Efficient interactive annotation of segmentation datasets with Polygon-RNN++. In *CVPR*, 2018.
- Michela Antonelli, Annika Reinke, Spyridon Bakas, Keyvan Farahani, Annette Kopp-Schneider, Bennett A Landman, Geert Litjens, Bjoern Menze, Olaf Ronneberger, Ronald M Summers, et al. The medical segmentation decathlon. *Nature communications*, 13(1):4128, 2022.
- Gustav Bredell, Christine Tanner, and Ender Konukoglu. Iterative interaction training for segmentation editing networks. In *Machine Learning in Medical Imaging: 9th International Workshop, MLMI 2018, Held in Conjunction with MICCAI 2018, Granada, Spain, September 16, 2018, Proceedings 9*, pages 363–370. Springer, 2018.
- Hu Cao, Yueyue Wang, Joy Chen, Dongsheng Jiang, Xiaopeng Zhang, Qi Tian, and Manning Wang. Swin-Unet: Unet-like pure transformer for medical image segmentation. In *ECCV Workshops Computer Vision*, 2023.
- Lluis Castrejon, Kaustav Kundu, Raquel Urtasun, and Sanja Fidler. Annotating object instances with a Polygon-RNN. In *CVPR*, 2017.
- Dongjie Cheng, Ziyuan Qin, Zekun Jiang, Shaoting Zhang, Qicheng Lao, and Kang Li. Sam on medical images: A comprehensive study on three prompt modes. *arXiv preprint arXiv:2305.00035*, 2023.
- DeepMind. surface-distance, 2018. URL <https://github.com/google/deepmind/surface-distance>. GitHub repository.
- Ruining Deng, Can Cui, Quan Liu, Tianyuan Yao, Lucas W Remedios, Shunxing Bao, Bennett A Landman, Lee E Wheless, Lori A Coburn, Keith T Wilson, et al. Segment anything model (SAM) for digital pathology: Assess zero-shot segmentation on whole slide imaging. *arXiv preprint arXiv:2304.04155*, 2023.
- Lee R Dice. Measures of the amount of ecologic association between species. *Ecology*, 26(3): 297–302, 1945.
- Haoyu Dong, Hanxue Gu, Yaqian Chen, Jichen Yang, and Maciej A Mazurowski. Segment anything model 2: an application to 2d and 3d medical images. *arXiv preprint arXiv:2408.00756*, 2024.
- Sheng He, Rina Bao, Jingpeng Li, P Ellen Grant, and Yangming Ou. Accuracy of segment-anything model (SAM) in medical image segmentation tasks. *arXiv preprint arXiv:2304.09324*, 2023a.
- Yufan He, Vishwesh Nath, Dong Yang, Yucheng Tang, Andriy Myronenko, and Daguang Xu. Swinunetr-v2: Stronger swin transformers with stagewise convolutions for 3d medical image segmentation. In *International Conference on Medical Image Computing and Computer-Assisted Intervention*, pages 416–426. Springer, 2023b.

Mohammad Hesam Hesamian, Wenjing Jia, Xiangjian He, and Paul Kennedy. Deep learning techniques for medical image segmentation: achievements and challenges. *Journal of Digital Imaging*, 32:582–596, 2019.

Yuhao Huang, Xin Yang, Lian Liu, Han Zhou, Ao Chang, Xinrui Zhou, Rusi Chen, Junxuan Yu, Jiongquan Chen, Chaoyu Chen, et al. Segment anything model for medical images? *arXiv preprint arXiv:2304.14660*, 2023.

Fabian Isensee, Paul F Jaeger, Simon AA Kohl, Jens Petersen, and Klaus H Maier-Hein. nnU-Net: a self-configuring method for deep learning-based biomedical image segmentation. *Nature Methods*, 18(2):203–211, 2021.

Ge-Peng Ji, Deng-Ping Fan, Peng Xu, Ming-Ming Cheng, Bowen Zhou, and Luc Van Gool. SAM struggles in concealed scenes – empirical study on “segment anything”. *arXiv preprint arXiv:2304.06022*, 2023a.

Wei Ji, Jingjing Li, Qi Bi, Wenbo Li, and Li Cheng. Segment anything is not always perfect: An investigation of SAM on different real-world applications. *arXiv preprint arXiv:2304.05750*, 2023b.

Alexander Kirillov, Eric Mintun, Nikhila Ravi, Hanzi Mao, Chloe Rolland, Laura Gustafson, Tete Xiao, Spencer Whitehead, Alexander C. Berg, Wan-Yen Lo, Piotr Dollár, and Ross Girshick. Segment anything. *arXiv:2304.02643*, 2023.

Wenhao Li, Qisen Xu, Chuyun Shen, Bin Hu, Fengping Zhu, Yuxin Li, Bo Jin, and Xiangfeng Wang. Interactive medical image segmentation with self-adaptive confidence calibration. *arXiv preprint arXiv:2111.07716*, 2021.

Xuan Liao, Wenhao Li, Qisen Xu, Xiangfeng Wang, Bo Jin, Xiaoyun Zhang, Yanfeng Wang, and Ya Zhang. Iteratively-refined interactive 3d medical image segmentation with multi-agent reinforcement learning. In *CVPR*, 2020a.

Xuan Liao, Wenhao Li, Qisen Xu, Xiangfeng Wang, Bo Jin, Xiaoyun Zhang, Yanfeng Wang, and Ya Zhang. Iteratively-refined interactive 3d medical image segmentation with multi-agent reinforcement learning. In *Proceedings of the IEEE/CVF conference on computer vision and pattern recognition*, pages 9394–9402, 2020b.

Di Lin, Jifeng Dai, Jiaya Jia, Kaiming He, and Jian Sun. ScribbleSup: Scribble-supervised convolutional networks for semantic segmentation. In *CVPR*, 2016.

Jie Liu, Yixiao Zhang, Kang Wang, Mehmet Can Yavuz, Xiaoxi Chen, Yixuan Yuan, Haoliang Li, Yang Yang, Alan Yuille, Yucheng Tang, et al. Universal and extensible language-vision models for organ segmentation and tumor detection from abdominal computed tomography. *Medical Image Analysis*, page 103226, 2024.

Yihao Liu, Jiaming Zhang, Zhangcong She, Amir Kheradmand, and Mehran Armand. SAMM (segment any medical model): A 3D slicer integration to SAM. *arXiv preprint arXiv:2304.05622*, 2023.

Chaofan Ma, Qisen Xu, Xiangfeng Wang, Bo Jin, Xiaoyun Zhang, Yanfeng Wang, and Ya Zhang. Boundary-aware supervoxel-level iteratively refined interactive 3d image segmentation with multi-agent reinforcement learning. *IEEE Transactions on Medical Imaging*, 40(10):2563–2574, 2021.

Jun Ma and Bo Wang. Segment anything in medical images. *arXiv preprint arXiv:2304.12306*, 2023.

Zdravko Marinov, Paul F Jäger, Jan Egger, Jens Kleesiek, and Rainer Stiefelhagen. Deep interactive segmentation of medical images: A systematic review and taxonomy. *arXiv preprint arXiv:2311.13964*, 2023.

Christian Mattjie, Luis Vinicius de Moura, Rafaela Cappelari Ravazio, Lucas Silveira Kupssinskü, Otávio Parraga, Marcelo Mussi Delucis, and Rodrigo Coelho Barros. Exploring the zero-shot capabilities of the segment anything model (sam) in 2d medical imaging: A comprehensive evaluation and practical guideline. *arXiv preprint arXiv:2305.00109*, 2023.

Maciej A Mazurowski, Haoyu Dong, Hanxue Gu, Jichen Yang, Nicholas Konz, and Yixin Zhang. Segment anything model for medical image analysis: an experimental study. *arXiv preprint arXiv:2304.10517*, 2023.

Bjoern H Menze, Andras Jakab, Stefan Bauer, Jayashree Kalpathy-Cramer, Keyvan Farahani, Justin Kirby, Yuliya Burren, Nicole Porz, Johannes Slotboom, Roland Wiest, et al. The multimodal brain tumor image segmentation benchmark (brats). *IEEE transactions on medical imaging*, 34(10):1993–2024, 2014.

Sovesh Mohapatra, Advait Gosai, and Gottfried Schlaug. Brain extraction comparing segment anything model (SAM) and fsl brain extraction tool. *arXiv preprint arXiv:2304.04738*, 2023.

Martin Rajchl, Matthew CH Lee, Ozan Oktay, Konstantinos Kamnitsas, Jonathan Passerat-Palmbach, Wenjia Bai, Mellisa Damodaram, Mary A Rutherford, Joseph V Hajnal, Bernhard Kainz, et al. DeepCut: Object segmentation from bounding box annotations using convolutional neural networks. *IEEE Transactions on Medical Imaging*, 36(2):674–683, 2016.

Nikhila Ravi, Valentin Gabeur, Yuan-Ting Hu, Ronghang Hu, Chaitanya Ryali, Tengyu Ma, Haitham Khedr, Roman Rädle, Chloe Rolland, Laura Gustafson, Eric Mintun, Junting Pan, Kalyan Vasudev Alwala, Nicolas Carion, Chao-Yuan Wu, Ross Girshick, Piotr Dollár, and Christoph Feichtenhofer. Sam 2: Segment anything in images and videos. *arXiv preprint*, 2024.

Olaf Ronneberger, Philipp Fischer, and Thomas Brox. U-Net: Convolutional networks for biomedical image segmentation. In *MICCAI*, 2015.

Saikat Roy, Tassilo Wald, Gregor Koehler, Maximilian R Rokuss, Nico Disch, Julius Holzschuh, David Zimmerer, and Klaus H Maier-Hein. SAM.MD: Zero-shot medical image segmentation capabilities of the segment anything model. *arXiv preprint arXiv:2304.05396*, 2023.

Neeraj Sharma and Lalit M Aggarwal. Automated medical image segmentation techniques. *Journal of Medical Physics*, 35(1):3, 2010.

Chunlin Shen, Wen Li, Qiang Xu, et al. Interactive medical image segmentation with self-adaptive confidence calibration. *Frontiers in Information Technology and Electronic Engineering*, 24(9):1332–1348, 2023. doi: 10.1631/FITEE.2200299.

Gwangmo Song, Heesoo Myeong, and Kyoung Mu Lee. SeedNet: Automatic seed generation with deep reinforcement learning for robust interactive segmentation. In *CVPR*, 2018.

Yucheng Tang, Jie Liu, Zongwei Zhou, Xin Yu, and Yuankai Huo. Efficient 3d representation learning for medical image analysis. *World Scientific Annual Review of Artificial Intelligence*, 2:2450002, 2024.

Guotai Wang, Maria A Zuluaga, Wenqi Li, Rosalind Pratt, Premal A Patel, Michael Aertsen, Tom Doel, Anna L David, Jan Deprest, Sébastien Ourselin, et al. DeepIGeoS: A deep interactive geodesic framework for medical image segmentation. *IEEE Transactions on Pattern Analysis and Machine Intelligence*, 41(7):1559–1572, 2018.

Junde Wu, Rao Fu, Huihui Fang, Yuanpei Liu, Zhaowei Wang, Yanwu Xu, Yueming Jin, and Tal Arbel. Medical SAM adapter: Adapting segment anything model for medical image segmentation. *arXiv preprint arXiv:2304.12620*, 2023.

Ning Xu, Brian Price, Scott Cohen, Jimei Yang, and Thomas S Huang. Deep Interactive Object Selection. In *CVPR*, 2016.

Chunhui Zhang, Li Liu, Yawen Cui, Guanjie Huang, Weilin Lin, Yiqian Yang, and Yuehong Hu. A comprehensive survey on segment anything model for vision and beyond. *arXiv preprint arXiv:2305.08196*, 2023.

Kaidong Zhang and Dong Liu. Customized segment anything model for medical image segmentation. *arXiv preprint arXiv:2304.13785*, 2023.

Yichi Zhang and Rushi Jiao. How segment anything model (SAM) boost medical image segmentation? *arXiv preprint arXiv:2305.03678*, 2023.

Hong-Yu Zhou, Jiansen Guo, Yinghao Zhang, Lequan Yu, Liansheng Wang, and Yizhou Yu. nnFormer: Interleaved transformer for volumetric segmentation. *arXiv preprint arXiv:2109.03201*, 2021.

Tao Zhou, Yizhe Zhang, Yi Zhou, Ye Wu, and Chen Gong. Can SAM segment polyps? *arXiv preprint arXiv:2304.07583*, 2023.

Jiayuan Zhu, Yunli Qi, and Junde Wu. Medical sam 2: Segment medical images as video via segment anything model 2. *arXiv preprint arXiv:2408.00874*, 2024.

A. Visualization Results

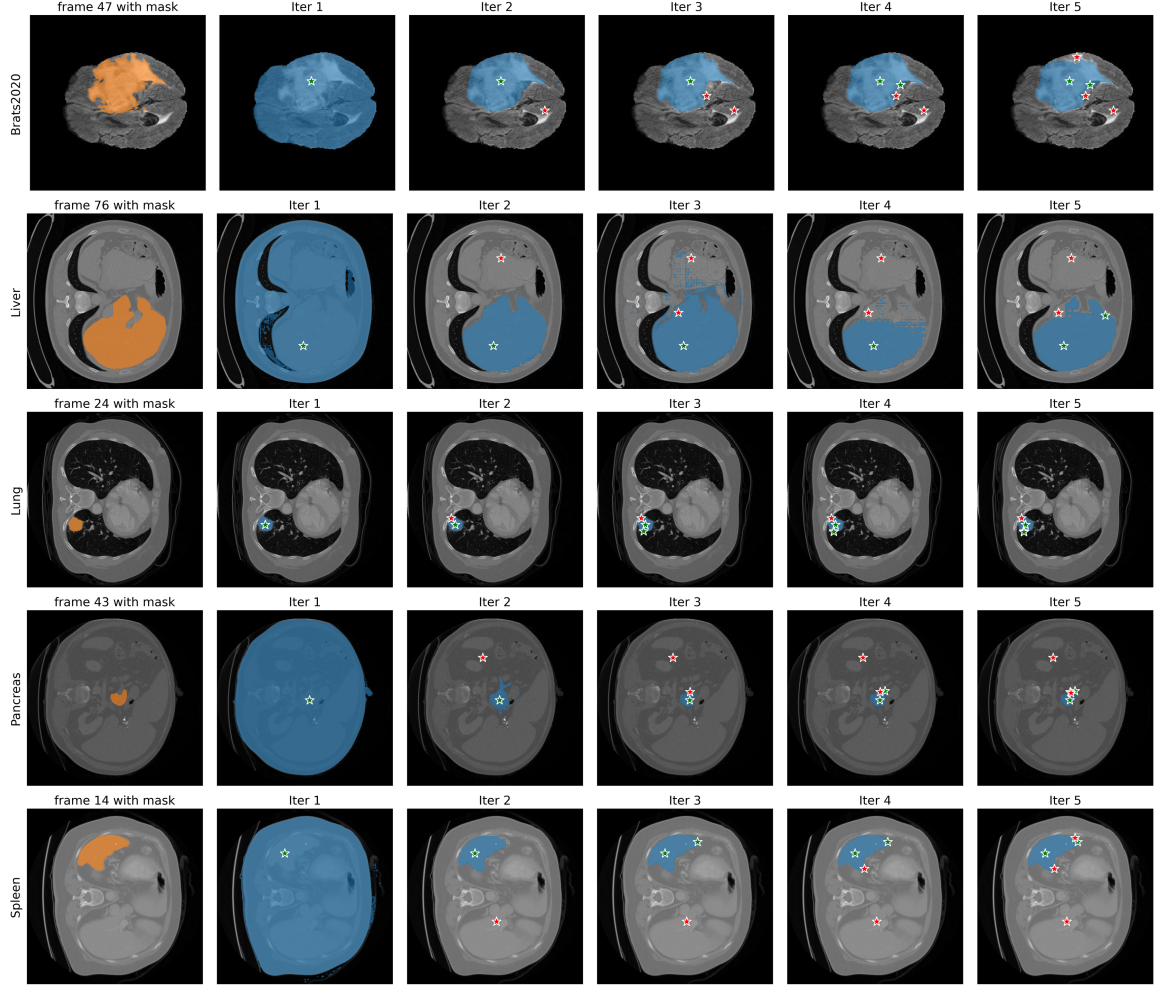


Figure A.1: SAM 2 segmentation 2D slices with 5 interactive clicks feedback. We show the ground truth mask as orange and the predicted mask as blue. We show foreground clicks in blue and background clicks in orange.

To further qualitatively study the accuracy of SAM 2 on medical images, we visualized the multi-round 2D slice interactive segmentation for brain tumors and different organs in Fig. A.1. Each row represents a different dataset, with the first column showing the Ground Truth, followed by the results of each subsequent round. It can be observed that SAM 2 effectively refines the results gradually, producing masks that closely resemble the ground truth.

Furthermore, using the interactive masks obtained from the fifth round, we applied SAM 2 to propagate the segmentation across the entire 3D image. The results on different datasets are shown in Fig. A.2. Each row represents a different dataset, with odd-numbered columns showing the ground truth of corresponding slices, followed by the predicted masks. Significant differences can be seen between slices of the 3D image, indicating substantial morphological

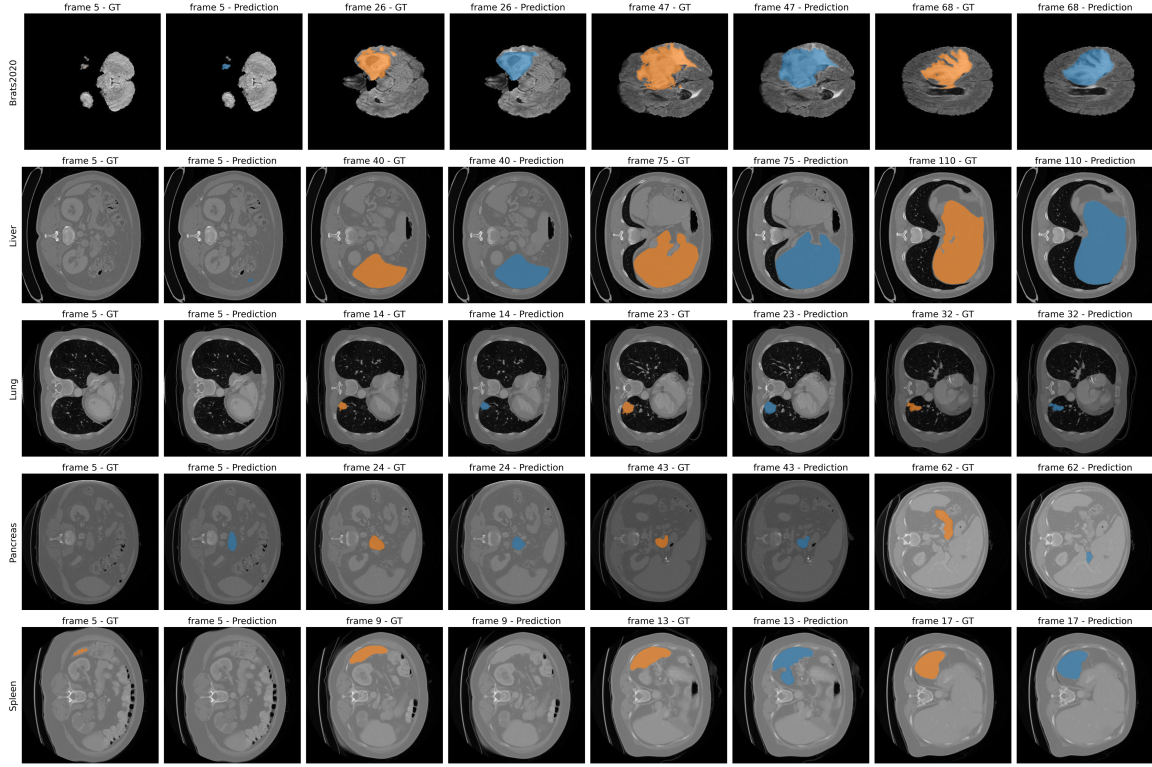


Figure A.2: Propagation: We show the ground truth mask as orange and the predicted mask as blue.

variations. In most cases, SAM 2 demonstrates good performance, although there are some failures, such as the last column in the spleen segmentation task, where the target regions in earlier slices were not identified by SAM 2.

These visual results demonstrate the zero-shot capability of SAM 2, which can achieve relatively accurate segmentation on medical images despite the significant differences from natural images. However, the precision of the segmentation still requires further improvement.